

THE CANADIAN MINERALOGIST

JOURNAL OF THE MINERALOGICAL ASSOCIATION OF CANADA

Volume 26

June 1988

Part 2

Canadian Mineralogist
Vol. 26, pp. 249-268 (1988)

UNCONFORMITY-RELATED URANIUM MINERALIZATION, McCLEEN DEPOSITS, NORTH SASKATCHEWAN, CANADA: HYDROGEN AND OXYGEN ISOTOPE GEOCHEMISTRY

COLIN J. BRAY AND EDWARD T.C. SPOONER

Department of Geology, University of Toronto, Toronto, Ontario, M5S 1A1

FREDERICK J. LONGSTAFFE*

Department of Geology, University of Alberta, Edmonton, Alberta, T6G 2E3

ABSTRACT

The McCleen uranium deposits in northern Saskatchewan consist of two linear zones of pods totalling 390,000 tonnes of ore (geological reserve) at 1.8% U_3O_8 above a 0.15% U_3O_8 cut-off. Mineralization is confined to within about +35 to -17m of the basal unconformity and is closely associated with narrow, fractured zones of basement graphitic (~25-45%) metasediments. The hydrogen and oxygen isotope geochemistry of illite from recrystallized sedimentary layers away from mineralization, and of illite from altered basement ("regolith") also away from mineralization, indicates that: (i) the original Athabasca sequence pore fluid had the isotopic characteristics of a typical, modern formation water ($\delta D \sim -45\text{‰}$, $\delta^{18}O \sim +6\text{‰}$); (ii) the high salinity of the formation-water was produced by evaporite dissolution, and not significantly by incorporation of bitterns, a deduction consistent both with the equatorial location ($<30^\circ$) of northern Saskatchewan between ~1450 Ma and ~1300 Ma, and with the presence of evaporite solution-collapse breccias in the overlying Carswell Formation; and (iii) altered basement ("regolith") either isotopically re-equilibrated with the original Athabasca formation-water or was produced by formation-

water/basement interaction. The "diagenetic-hydrothermal" hypothesis for the origin of Canadian unconformity-related uranium mineralization is supported by the following evidence: (i) the $\delta^{18}O$ values of the fluids involved in a hydrothermal alteration halo around mineralization and in "bleached"-facies mineralization are the same as those estimated for the original Athabasca formation-water ($\sim +5\text{‰}$ to $\sim +10\text{‰}$); (ii) selective D depletion of fluids from the alteration-halo/"bleached" facies of mineralization to δD values as low as -125‰ can be interpreted as having resulted from modification by low δD $CO_2 \pm CH_4 \pm H_2S \pm H_2$ derived by interaction with basement graphitic metasediments; (iii) D depletion of fluids from the alteration-halo/"bleached" facies has a statistically significant correlation with U_3O_8 grades and with laser-probe $^{40}Ar/^{39}Ar$ and conventional K/Ar dates; (iv) fluids from the arsenide/sulfide facies of mineralization show D depletion and also a marked positive $\delta^{18}O$ shift from Athabasca formation-water $\delta^{18}O$ values to values as high as $\sim +18\text{‰}$; the latter trend is interpreted to have resulted from formation-water - basement oxygen isotope exchange; and (v) the $\delta^{18}O$ values of carbonate from veins beneath mineralization (9-22 m below the unconformity) show that a high $\delta^{18}O$ fluid ($\sim +6\text{‰}$ to $\sim +17\text{‰}$) did evolve in fractured basement.

* Present address: Department of Geology, University of Western Ontario, London, Ontario, N6A 5B7

Keywords: uranium, isotopes, hydrogen, oxygen, Saskatchewan.

SOMMAIRE

Les gisements d'uranium de McClean, dans le nord de la Saskatchewan, contiennent des réserves de 390,000 tonnes de minerai à teneur en U_3O_8 de 1.8% (seuil de 0.15% $U_3O_8 \cdot m$) en lentilles étalées sur deux zones linéaires. La minéralisation est limitée à une bande allant de +35 à -17 m de la discordance à la base de la séquence; elle est associée à des zones étroites de fissures dans les sédiments graphitiques (25-45%) du socle. La géochimie isotopique (oxygène et hydrogène) de l'illite des niveaux métasédimentaires recristallisés et du socle altéré ("régolithe"), tous deux éloignées de la minéralisation, montre que: (i) la phase fluide des pores de la séquence Athabasca originelle a les caractéristiques isotopiques d'une eau de gisement moderne typique ($\delta D = -45\%$, $\delta^{18}O = +6\%$); (ii) la salinité élevée de l'eau de gisement résulte de la dissolution d'évaporite, et non pas de l'incorporation importante de saumures. Cette déduction est en accord à la fois avec la latitude équatoriale ($<30^\circ$) du nord de la Saskatchewan entre 1450 et 1300 Ma environ, et le développement de brèches d'effondrement dans la séquence supérieure des évaporites de la formation Carswell; (iii) le socle altéré ("régolithe") est isotopiquement ré-équilibré avec l'eau de gisement de la séquence Athabasca originelle, ou bien résulte d'une interaction entre l'eau de gisement et le socle. Les facteurs suivants favorisent une origine "diagenétique-hydrothermale" pour les gisements canadiens d'uranium liés à une discordance: (i) les valeurs de $\delta^{18}O$ des fluides qui ont produit une auréole d'altération hydrothermale autour des zones minéralisées ainsi qu'un facies blanchi de la minéralisation sont celles de l'eau de gisement de la séquence Athabasca originelle (environ +5 à +10‰); (ii) un appauvrissement sélectif en D des fluides impliqués dans l'auréole d'altération et dans le facies blanchi de la zone minéralisée, jusqu'à des valeurs de δD de -125‰, résulterait de modifications par des fluides riches en $CO_2 \pm CH_4 \pm H_2S \pm H_2$, à faible δD , dérivés des métasédiments graphitiques du socle; (iii) la diminution en D des fluides des facies altérés montre une corrélation statistiquement significative avec les teneurs en U_3O_8 , les rapports $^{40}Ar/^{39}Ar$ obtenus par sonde au laser, et les datations K/Ar obtenues de façon conventionnelle; (iv) les fluides du facies riche en arséniures et en sulfures ont subi une diminution de la teneur en D ainsi qu'une augmentation importante en O^{18} , au delà des valeurs de l'eau de gisement, jusqu'à des valeurs de $\delta^{18}O$ de +18‰; l'enrichissement en O^{18} résulterait d'un échange isotopique entre l'eau de gisement et le socle; (v) les valeurs de $\delta^{18}O$ des carbonates de fissures situées en dessus des zones minéralisées (de 9 à 22 m en dessous de la discordance) indiquent qu'un fluide à $\delta^{18}O$ élevé (environ +6 à +17‰) a effectivement eu une origine dans le socle fissuré.

(Traduit par la Rédaction)

Mots-clés: uranium, isotopes, hydrogène, oxygène, Saskatchewan.

INTRODUCTION

In 1984 Canada became the largest market-economy-country uranium producer in the world. Output was 11,170 tonnes U, a 55% increase over

1983 (Table 1). Output for 1986 was forecast to be 11,770 tonnes (NUKEM Market Report 1986). The unconformity-related deposits in the Proterozoic Athabasca basin of N. (northern) Saskatchewan are largely responsible for this position since they now account for 55% of total Canadian production, the remainder coming almost completely from the Elliot Lake area (Mining Annual Review 1985). As an example, the Key Lake operation which started processing ore in October, 1983, has become the world's largest uranium production center at a designed capacity of 4,600 tonnes U per annum (Mining Annual Review 1985).

Since the discovery of the Rabbit Lake and Cluff Lake uranium deposits in 1968 and 1969, the Proterozoic Athabasca sedimentary basin, where the N. Saskatchewan deposits are located, has been found to contain several large orebodies. For example, Cigar Lake and Key Lake (discovered in 1981 and 1975-76) are the world's fourth and sixth largest known uranium deposits for which reliable data are available (see Bray *et al.* 1987 for compilation). They contain 177,000 and 89,120 tonnes U_3O_8 , respectively. The N. Saskatchewan deposits are unusual because of their high grades and, therefore, low actual or potential production costs. As examples, the Key Lake deposit averages 2.4% U_3O_8 and the Cigar Lake main pod, which contains 74% of the total Cigar Lake geological reserve, averages 14% U_3O_8 . Among the world's six largest known uranium deposits (Bray *et al.* 1987) that with the next highest grade is Jabiluka Two (#3) in Australia at 0.39% U_3O_8 . The largest, Olympic Dam (Australia), contains only ~0.06% U_3O_8 .

The unconformity-related deposits in N. Saskatchewan are thought to have formed by a "diagenetic-hydrothermal" process in which U^{VI} , carried in a relatively oxidizing formation water in the Athabasca Basin sequence, was precipitated as U^{IV} compounds by reaction with reductant produced by formation-water interaction with fractured graphitic metasediments in the basement (Hoeve & Sibbald 1978, Hoeve *et al.* 1980, Sibbald *et al.* 1981). The aim of the work presented here was to test this hypothesis by examining a specific case-history in detail (Bray *et al.* 1982, 1984, 1987). Although relatively small (7,020 tonnes contained U_3O_8), the McClean group of deposits located 11 km west-northwest of the Rabbit Lake mine (Fig. 1) has turned out to be a good choice for the following reasons: (i) the group lies in the middle of an area containing at least seven other similar uranium discoveries, including Cigar Lake, the most important cluster defined to date in N. Saskatchewan (Fogwill 1985, Fouques *et al.* 1986; Fig. 1), (ii) the geological characteristics and relationships of the McClean mineralization are very similar to those of larger deposits such as Cigar Lake (Fouques *et al.* 1986; see below), Key Lake (Dahlkamp 1978) and

Midwest (Wray *et al.* 1985), (iii) the McClean deposits occur everywhere beneath ~150 m of Athabasca sandstone, which is very well lithified in places and which has thus protected the deposits from chemical weathering (Wallis *et al.* 1984) and (iv) the geological characteristics and relationships of the McClean deposits have been documented thoroughly (Wallis *et al.* 1983, 1984, 1985).

GEOLOGICAL CHARACTERISTICS

The McClean deposits were only the second to be found in N. Saskatchewan without the presence of visible surface mineralization either as float or outcrop. Discovery of the McClean North Zone by a Canadian Occidental Petroleum (Minerals Division)/INCO Metals Company joint ventureship was

TABLE 1. MARKET ECONOMY COUNTRY URANIUM PRODUCTION, 1983 - 1986

Country (listed in 1984 order of production)	Production (metric tonnes U)			
	1983	1984	1985 (estimated)	1986 (forecast)
Canada	7,200	11,170	11,290	11,770
United States	8,200	5,920	4,510	4,255
Republic of South Africa	6,100	5,780	4,780	4,660
Australia	3,200	4,310	3,680	3,680
Namibia/S.W. Africa	3,800	3,620	3,650	3,650
Other Africa (Niger and Gabon)	4,400	4,400	4,220	4,350
Other	4,500	4,000	4,020	4,615
Totals	37,400	39,200	36,150	36,980

Figures from Mining Annual Review 1984 (p. 85), Mining Annual Review 1985 (p. 109) and NUKEM Market Report 1/86 (p.10).

confirmed in March, 1979 by drilling an "under-snow" three-station radon anomaly located above

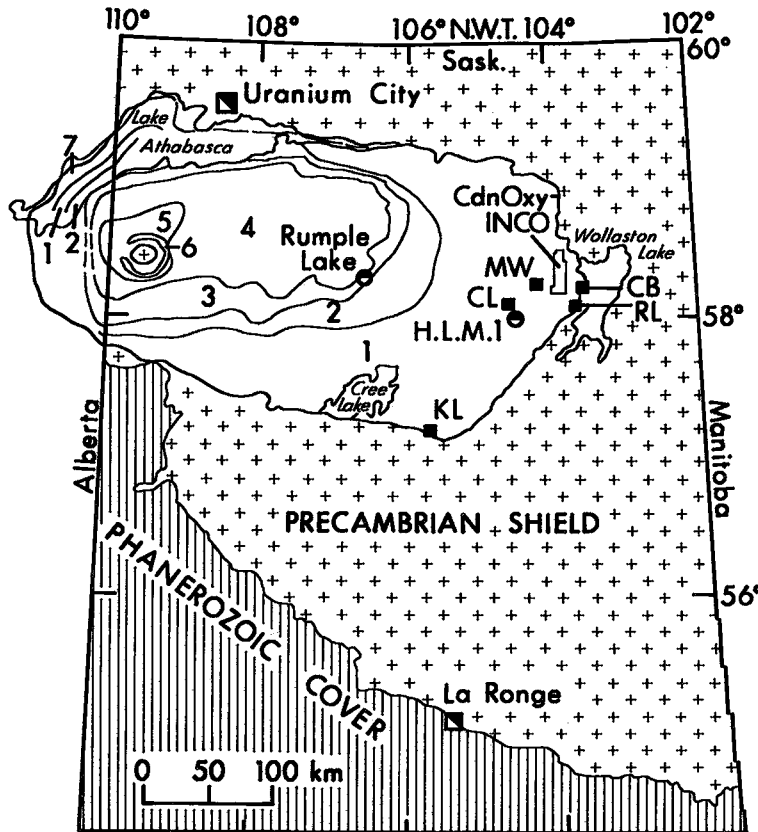


FIG. 1. Location map of the Athabasca Basin, northern Saskatchewan showing the distribution of the five main known uranium deposits in the eastern part of the basin in relation to the Canadian Occidental/INCO property, the southwestern part of which contains the McClean deposits (see Fig. 5), and the surface extents of the different Athabasca sandstone units. CB Collins Bay, CL Cigar Lake, KL Key Lake, MW Midwest, RL Rabbit Lake. Athabasca sequence formation names: 1 Manitou Falls; 2 Wolverine Point; 3 Locker Lake; 4 Otherside; 5 Tuma Lake; 6 Carswell and Douglas; 7 Fair Point (after Armstrong & Ramaekers 1985). The locations of the Rumpole Lake and H.L.M.1 stratigraphic boreholes are also shown.

a MaxMin EM conductor (hole 153-79 which intersected 7.51% U_3O_8 over 10.1 m; Saracoglu *et al.* 1983). The South Zone was discovered on January 14, 1980 by systematic drilling of another EM conductor. Finally, 426 holes in the two zones defined a combined geological reserve (1981) of 390,000 tonnes at a weighted average grade of 1.8% U_3O_8 above a 0.15% U_3O_8 .m cut-off (Wallis *et al.* 1983).

Mineralization and associated hydrothermal alteration occur as two linear zones of elongate pods with sharp grade boundaries (0.15% U_3O_8 .m cut-off; Fig. 2). The North Zone, which contains 72% of the

contained uranium, consists of four separate pods totalling ~ 730 m in length, and averaging ~ 15-46 m in width and ~ 2-20 m in height (e.g., Fig. 3 showing pods N2-N4). The South Zone consists of two pods ~ 220 - 280 m long. Mineralization is highly variable in intensity, can be very high grade (e.g., 27.8% U_3O_8 over 10.1 m), and is tightly confined to within +35 m/-17 m of the basal unconformity between the middle Proterozoic Athabasca sequence (units B and C of the Manitou Falls Formation; Ramaekers 1981) and the Archean - Aphebian (Lower Proterozoic) basement. This mode of

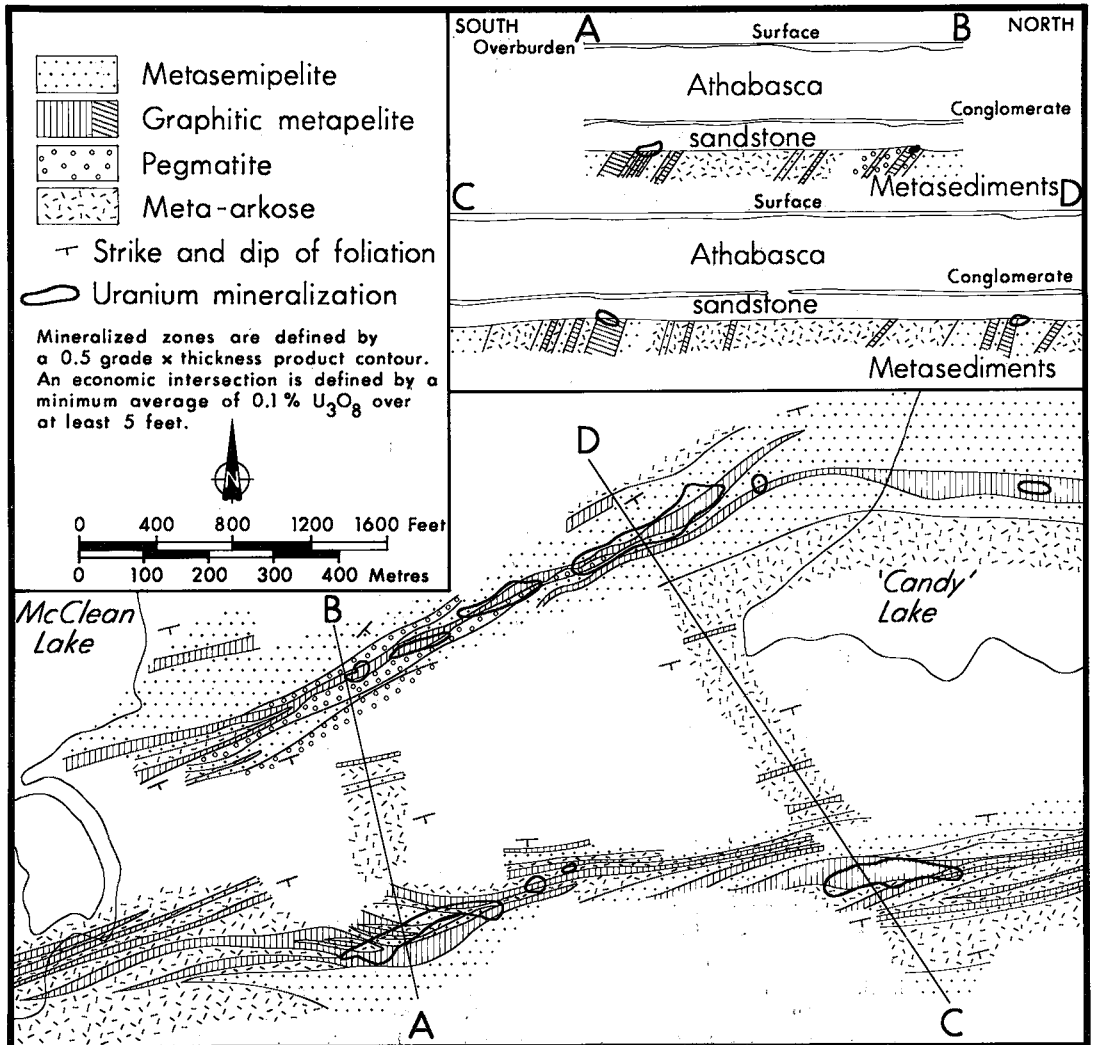


FIG. 2. Plan and sections of the McClean uranium deposits showing the elongate pods of mineralization located at the basal unconformity, and the spatial relationship between uranium mineralization and graphitic metasediments in the basement (modified from Wallis *et al.* 1984, 1985). Feet are used for grade x thickness contours because all drilling and ore-reserve calculations before 1981 for McClean deposits used Imperial (British) units (e.g., Wallis *et al.* 1985).

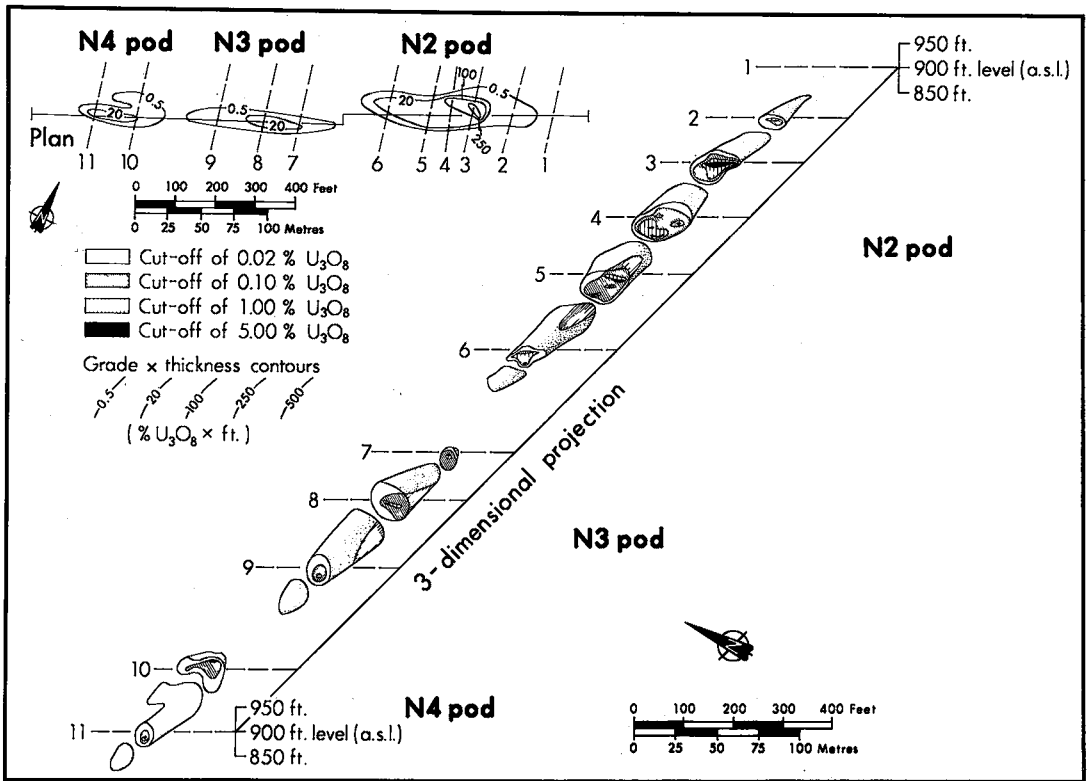


FIG. 3. Three-dimensional representation and grade \times thickness contoured plan of McClean North Zone pods N2-N4 to illustrate the elongate and pod-like distribution of the mineralization (modified from an original supplied by the Canadian Occidental Petroleum Ltd./INCO Metals Co. joint ventureship; a similar diagram of pod N1 is given in Wallis *et al.* 1984, 1985).

occurrence is characteristic of many of these deposits (e.g., Cigar Lake, Fouques *et al.* 1986; Key Lake, Dahlkamp 1978; Midwest, Wray *et al.* 1985).

The basement in the McClean area consists of meta-arkoses, meta semi-pelites and segregation pegmatites (Fig. 2; Wallis *et al.* 1983). A "regolith" occurs immediately below the unconformity which is thought to have formed either as a paleoweathering profile of lateritic character before Athabasca sedimentation (MacDonald 1985), or by diagenetic processes after Athabasca sedimentation, or by a combination of both processes (Bray *et al.* 1987).

Mineralization is situated within and just above semi-pelite units which typically contain 25-45%, and occasionally 80%, graphite (Fig. 2). Fractures and breccias occur in the basement rocks below and within mineralization. More numerous fractures occur in the overlying sandstone above mineralization. For example, fractures in the North Zone occur in an area 45 m wide, 915 m long, and up to 150 m thick. Mineralization is, therefore, clearly controlled by highly graphitic horizons in the basement and by abundant fractures below and above the unconformity. An important point is that graphite immedi-

ately beneath mineralization shows clear evidence of reaction; it is recrystallized to a fine-grained, "sooty" material and, above all, shows pronounced depletion zones (Wallis *et al.* 1983, 1984).

Mineralized rocks contain four principal mineral assemblages: sulfide, arsenide, "bleached", and hematite facies. The sulfide and arsenide facies are differentiated by the relative abundances of pyrite-bravoite to Ni-Co arsenides such as nickeline (NiAs), pararammelsbergite (NiAs₂), and gersdorffite (Ni,Co,Fe)AsS. Contacts are gradational, with the sulfide facies overlying the arsenide facies. Colloform pitchblende, euhedral uranium oxide, coffinite (USiO₄)(OH)₄, ferrous chlorite, siderite, illite, chalcocopyrite, sphalerite and galena are common to both facies (Wallis *et al.* 1983, 1984, 1985). The bleached and hematitic facies are characterized by black, ~5 mm to ~5 cm nodules of pitchblende \pm coffinite, pararammelsbergite, nickeline, and gersdorffite set either in a light-colored illite matrix ("bleached" facies), or in an illite matrix impregnated with hematite or goethite (or both) (hematite facies; Wallis *et al.* 1983, 1984). The illite was produced by hydrothermal alteration since it clearly

replaced both Athabasca sandstone and basement material, quartz grains in the former being clearly corroded. Illite as part of a hydrothermal alteration halo typically occurs 60 m above mineralization and up to 150 m above some high-grade intersections. Textural evidence suggests that all four mineral facies are broadly cogenetic, but that formation of sulfide and arsenide facies may have started earlier, and formation of "bleached" and hematite facies may have persisted later. These relationships are important because the hydrogen and oxygen isotope characteristics of both chlorite and illite ("bleached" facies of mineralization and alteration halo) have been examined in this study.

As mentioned above, the McClean deposits are small, even collectively. However, the mineralization

at McClean is remarkably similar to that at the large, high grade, Cigar Lake discovery located only 47 km to the southwest. Hence, it is possible that findings at McClean may be applicable to Cigar. The similarities are as follows (information from Fouques *et al.* 1986): (i) mineralization is elongate (length ~1800 m), relatively narrow (~25–105 m), and relatively thin (~5–30 m) (Fig. 4a and b), (ii) mineralization is pod-like (Fig. 4b) and can be very high grade (e.g., 37.7% U_3O_8 over 19 m), (iii) the bulk of the mineralization is located as a lens (Fig. 4c) at the basal unconformity (+25 m, -10 m), although some examples of perched mineralization were intersected up to 200 m above the unconformity, (iv) the orebody is directly related to a DEEPEM conductor found to consist of graphitic (~3–10%), sulfide-

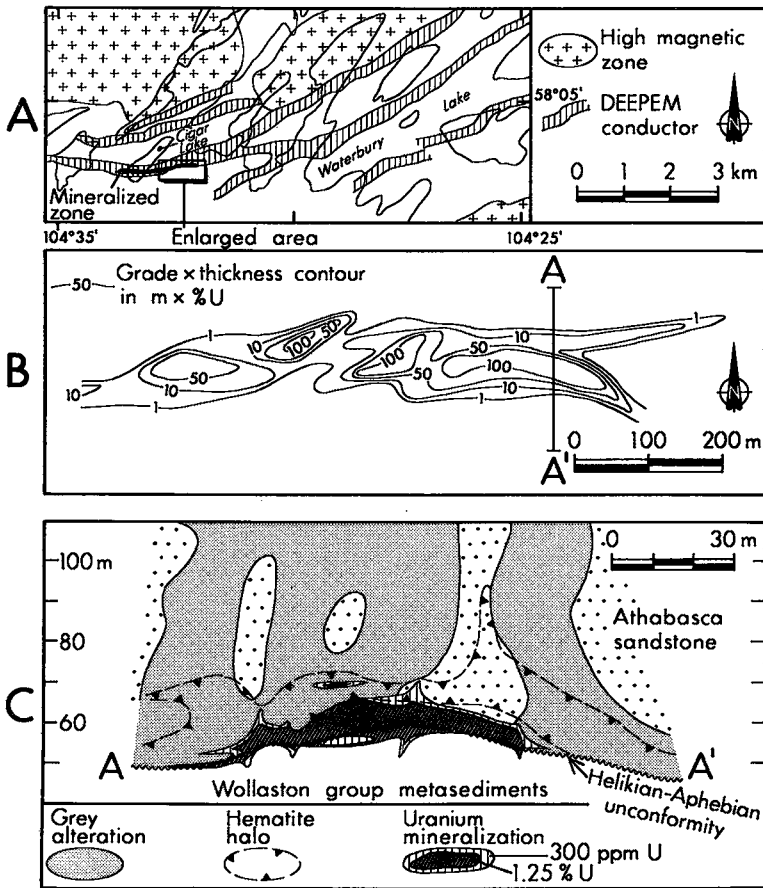


FIG. 4. Cigar Lake uranium deposit (modified from Fouques *et al.* 1986). (A) The 1.8 km-long mineralized zone showing its linearity and spatial relationship to a graphitic DEEPEM conductor. (B) Contoured grade \times thickness contours of the Cigar Lake East zone showing the pod nature of the mineralization. (C) Vertical section of the Cigar Lake East Zone along the section line given in (B) showing the thin lens of mineralization located exactly at ($\sim +25$ m to -10 m) the basal unconformity above graphitic (~ 3 – 10%), sulfide-bearing (~ 1 – 5%) augen gneiss.

bearing (~1–5%) augen gneiss (Fig. 4a), (v) the immediate subjacent basement is faulted (2 sets) with some fracture zones controlling hydrothermal alteration, (vi) the mineralization consists of uraninite, pitchblende, later coffinite, pyrite-bravoite, a suite of Ni–Co arsenides and sulfarsenides, a suite of Cu, Zn and Pb sulfides, and a complex sheet silicate – siderite gangue, (vii) the deposit is surrounded by an intense clay-alteration halo, extending above mineralization for as much as 200 m, which consists predominantly of illite (up to ~30%), and an illite–chlorite envelope immediately around mineralization, and (viii) within the upper few meters of basement alteration beneath mineralization is a graphite-depletion zone which contains carbonaceous “globules”.

SAMPLE DESCRIPTIONS AND ANALYTICAL PROCEDURES

Since the objective of this work was to test the “diagenetic-hydrothermal” hypothesis for the origin of the unconformity-related uranium deposits in

N. Saskatchewan (Hoeve & Sibbald 1978, Hoeve *et al.* 1980, Sibbald *et al.* 1981) the δD and $\delta^{18}O$ values of a variety of mainly secondary materials have been determined in order to characterize the original hydrogen and oxygen isotope geochemistry of pore fluids in the Athabasca sandstone sequence, fluids which interacted with basement away from mineralization, fluids involved in the hydrothermal alteration halo around mineralization, fluids involved in both principal types of mineralization (arsenide/sulfide and “bleached”/hematite facies), and also fluids which interacted with basement beneath mineralization. Analyzed materials thus include:

(i) Recrystallized sedimentary-layer illite away from mineralization ($n = 4$; as many as were obtainable) with K/Ar and laser probe $^{40}Ar/^{39}Ar$ dates of 1485 ± 55 Ma (1σ) – 1130 ± 1 Ma ($n = 5$), which are closely similar to dates of 1459 ± 4 Ma – 1113 ± 11 Ma ($n = 3$) for clearly secondary diagenetic illite interstitial to sandstone quartz grains (age data from Bray *et al.* 1987). Sample locations are given in the appendix and in Figure 5, and data are given in

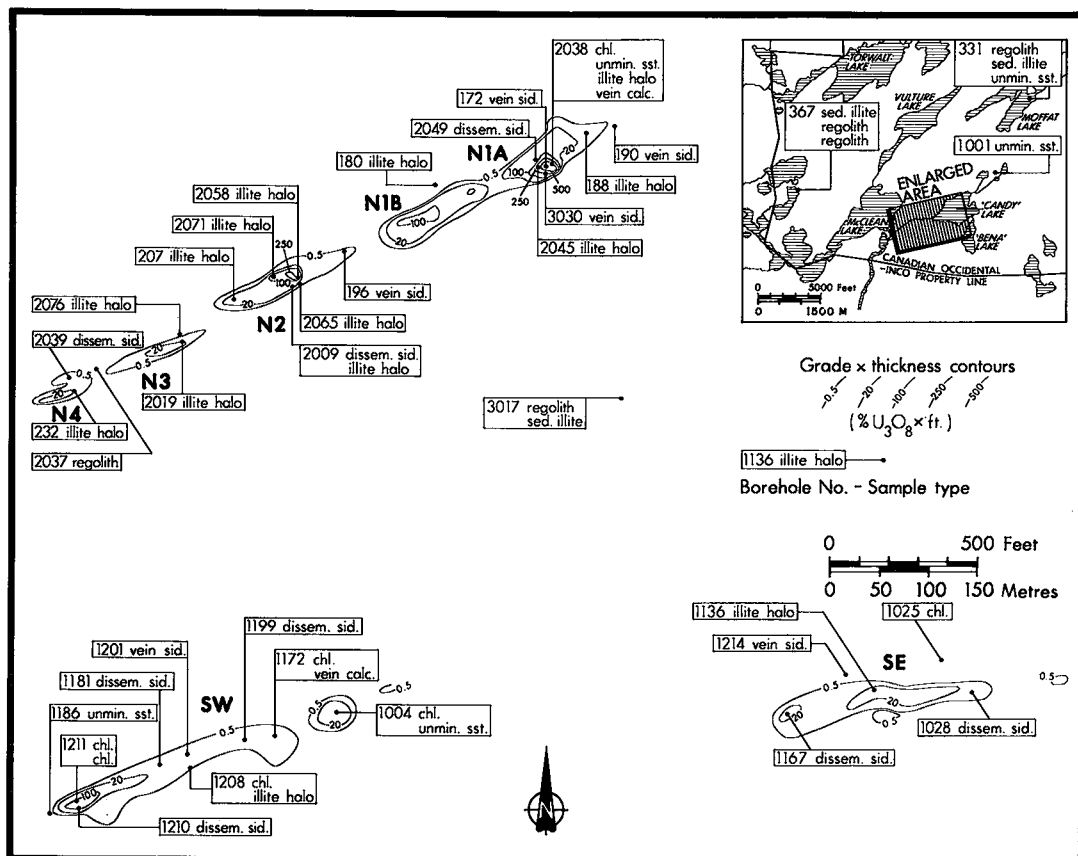


FIG. 5. Sample location maps. Drafted from Canadian Occidental Petroleum Ltd./INCO Metals Co. base maps.

Table 2. HYDROGEN AND OXYGEN ISOTOPE RATIOS OF SECONDARY ILLITE AND TYPICAL ATHABASCA SANDSTONE

Sample number (borehole number and depth in feet)	δD (‰) (SMOW)	$\delta^{18}O$ (‰) (SMOW)
<u>Recrystallized sedimentary clay layers in Athabasca sandstone away from known uranium mineralization</u>		
3017 - 145	-66, -66*	+11.2
367 - 487	-70	+11.0
375 - 502	-76	+ 9.5
331 - 244	-66	+11.0
<u>Illite pseudomorphs of primary feldspar in altered basement ("regolith") away from mineralization.</u>		
2037 - 599	-82	+12.2
3017 - 537.5	-64	+15.3
367 - 677.5	-69	+11.5
367 - 713.5	-65	+ 9.2
371 - 603.5	-76	+10.5
331 - 379	-80	+11.0
<u>Secondary illite from the hydrothermal alteration halo and from the "bleached" facies of uranium mineralization</u>		
188 - 541	-103	+11.5
2038 - 529	-137	+11.0
2045 - 523	-103	+10.6
180 - 527	-65	+11.3
2058 - 550	-135	+13.4
2009 - 526	-115	+11.4
2065 - 375	-79, -76*	+10.9
2071 - 486	-77	+ 9.5
207 - 533	-100, -104*	+10.8
2019 - 541	-147, 152*	+14.4
2076 - 487	-79	+10.0
232 - 513	-114	+10.1
1136 - 499	-138, -143, -144*	+13.0
1208 - 458	-73	+10.2
<u>Typical unmineralized Athabasca sandstone</u>		
2038 - 259.5	-	+ 9.9
1004 - 407	-	+10.0
1186 - 460	-	+11.4
1001 - 256	-	+10.0
331 - 87	-	+ 9.7
Mean $\pm 1\sigma$	-	+10.2 \pm 0.7

* Results for separate vacuum extractions from the same sample.

Table 2. Samples are from up to 5 km from known mineralization, and from between 0.5 m and 118 m above the unconformity.

(ii) Secondary illite from feldspar pseudomorphs in altered basement ("regolith") away from mineralization ($n = 6$) which give K/Ar ages of 1482 ± 49 Ma - 1262 ± 44 Ma ($n = 6$), closely comparable to those obtained from interstitial diagenetic illite and illite from recrystallized sedimentary layers (see above). Samples are from up to 5 km from known mineralization and from up to 33 m below the unconformity (Appendix and Fig. 5).

(iii) Illite from hydrothermally altered rocks surrounding mineralization, and from the "bleached" facies of mineralization ($n = 14$; Table 2). Exact sample locations are given in the appendix, and in Figure 5 which shows outlines of the pods. Most samples (12) were obtained from the North Zone as it contains the best developed "bleached"/hematite facies mineralization. Laser probe $^{40}Ar/^{39}Ar$ ($n = 10$) and K/Ar ($n = 10$) dates for this type of material show a sharp beginning at ~ 1320 Ma, a peak in the 1250-1150 Ma age bracket, and a tail to dates as young as 1002 ± 33 Ma (Bray *et al.* 1987). These dates show significant overlap with the ages of the illites discussed in categories (i) and (ii) above, falling in the younger part of the range.

(iv) Secondary chlorite samples from the arsenide and sulfide facies of mineralization ($n = 7$; Table 3, Fig. 5) most of which (6) are from the South Zone where these facies are developed best. Estimation of the chlorite $\delta^{18}O$ values (see bottom of Table 3) required determination of the oxygen isotopic composition of typical unmineralized Athabasca sandstone samples ($n = 5$; Table 2).

Table 3. MEASURED WHOLE ROCK HYDROGEN ISOTOPE RATIOS (= CHLORITE), SiO_2 , Al_2O_3 , MgO AND TOTAL Fe AND FeO CONTENTS, MEASURED WHOLE ROCK OXYGEN ISOTOPE RATIOS AND CALCULATED CHLORITE OXYGEN ISOTOPE RATIOS FOR THE CHLORITIC SULFIDE AND ARSENIDE FACIES OF URANIUM MINERALIZATION. (ALL SAMPLES ARE MINERALIZED SANDSTONES).

Sample number (borehole number and depth in feet)	Sample location	δD whole rock, measured (‰; SMOW)	SiO_2 (wt.%)	Al_2O_3 (wt.%)	MgO (wt.%)	Total Fe as FeO (wt.%)	Total SiO_2 + Al_2O_3 + MgO (wt.%)	$\delta^{18}O$ whole rock, measured (‰; SMOW)	$\delta^{18}O$ chlorite calculated* (‰; SMOW)
2038 - 534	McClellan N1A	-139	78.8	4.59	0.38	4.70	88.5	+11.2	+18
1004 - 542	McClellan SW	-131	61.5	10.2	0.65	7.20	79.6	+10.9	+13
1172 - 545	McClellan SW	-124	84.3	5.7	0.24	1.21	91.5	+9.9	+7
1208 - 542	McClellan SW	-100	66.9	4.16	1.31	11.96	84.3	+8.8	+5
1211 - 505	McClellan SW	-121	69.5	5.97	0.17	6.26	81.9	+9.2	+4
1211 - 528	McClellan SW	-127	79.6	7.34	0.40	2.59	89.9	+10.8	+15
1025 - 540	McClellan SE	-131, 139†	56.1	13.5	1.01	9.71	80.3	+12.3	+17

*Calculated assuming that SiO_2 , Al_2O_3 , MgO and FeO are, to a first approximation, contained only in quartz and chlorite, that the total numbers of aluminium ions in octahedral and tetrahedral sites in chlorite are equal for charge balance reasons, which implies that the concentration of Fe^{3+} is small compared with Fe^{2+} , and that relict quartz grains have not exchanged oxygen isotopes to any significant degree during mineralization so that a $\delta^{18}O$ value for relict quartz is given by the mean ($\pm 1\sigma$) for five Athabasca sandstone analyses ($+10.2\text{‰} \pm 0.7\text{‰}$; Table 2).

†Results for separate vacuum extractions from the same sample.

Analyst for major elements: X-Ray Assay Laboratories Ltd., 1885 Leslie St., Don Mills, Ontario, M3B 3J4 Canada

(v) Disseminated and vein carbonate samples (14 siderite; 2 calcite) from within the sulfide and arsenide facies of mineralization, and from veins in and below mineralization (Appendix, Table 4, Fig. 5). The five vein samples from beneath mineralization occur in graphitic metasediments up to 22 m below the unconformity.

Silicate δD , silicate $\delta^{18}O$ and calcite $\delta^{18}O$ values were determined, respectively, by Krueger Enterprises, Inc. (Geochron Laboratories Division), by F.J.L. at the Department of Geology, University of Alberta, and by the Isotope Laboratory, University of Waterloo, Ontario, using standard techniques. The 1σ uncertainties are $\pm 2\text{‰}$, $\pm 0.2\text{‰}$ and $\pm 0.2\text{‰}$. The siderite-bearing samples did not react significantly even after a week in contact with phosphoric acid at 25°C , probably because of the formation of an impermeable layer of iron phosphate. The $\delta^{18}O$ values of the siderite samples were determined by Dr. H.R. Krouse, Department of Geology, University of Calgary, by reaction with SnCl_2 at 300°C in a closed pyrex tube for 30 min. Standards were run alongside the unknowns because the latter method can give results up to 2‰ different from the phosphoric acid technique. The uncertainty was estimated to be $\pm 0.2\text{‰}$ (1σ).

ISOTOPE FRACTIONATION FACTORS AND THE TEMPERATURE FOR ESTIMATING FLUID δD AND $\delta^{18}O$ VALUES

The following isotope-fractionation factors were used to calculate fluid parameters:

- (i) δD (illite): Marumo *et al.* (1980) give four empirical sericite - water hydrogen isotope fractionation factors from the Ohnuma geothermal system in northeastern Japan which are similar within a $130\text{--}250^\circ\text{C}$ temperature range (-27.0 , -27.0 , -26.3 , -23.6). Hence, an arithmetic mean of -26.0 is taken.
- (ii) $\delta^{18}O$ (illite): Eslinger & Savin's (1973) empirical data from the Ohaki - Broadlands geothermal system in New Zealand are used.
- (iii) δD (chlorite): Marumo *et al.* (1980) report 21 empirical chlorite - water hydrogen isotope fractionations for temperatures between 130°C and 250°C . They suggested that there was a relationship between the fractionation factor and the $\text{Fe}/(\text{Fe} + \text{Mg})$ ratio of the chlorite without testing whether or not there was a coincidental correlation with temperature. As shown in Figure 6, there is a statistically significant correlation with $10^6 \cdot T^{-2}$, but no preferred relationship with $\text{Fe}/(\text{Fe} + \text{Mg})$. Interpretation of the temperature relationship is problematical, however, because the slope is positive, unlike all other known silicate - water hydrogen isotope fractionation curves

Table 4. OXYGEN ISOTOPE RATIOS OF CARBONATES

Sample number (borehole number and depth in feet)	CO ₂ contents of whole rock samples (wt.%)	$\delta^{18}O$ (‰) (SMOW)
<u>Fine grained disseminated siderite from the sulfide and arsenide facies of uranium mineralization</u>		
2049 - 534	1.2*	+20.4
2009 - 566	12.0†	+22.0
2039 - 529	5.7*	+18.4
1199 - 544	2.7†	+16.5
1181 - 546.5	5.5*	+23.8
1210 - 510	6.9†	+18.1
1028 - 542	4.5†	+15.2
1167 - 537 to 542	14.1*	+25.2
<u>Vein siderite from within and below mineralization</u>		
190 - 560	-	+21.4
172 - 510	-	+16.1
3030 - 507.3	-	+19.1
196 - 580	-	+22.7
1201 - 543.5	-	+21.5
1214 - 565	-	+23.6
<u>Vein calcite below mineralization</u>		
2038 - 602	-	+16.2
1172 - 598	-	+25.1

Analysts: CO₂, * INCO Ltd. and †X-Ray Assay Laboratories Ltd.

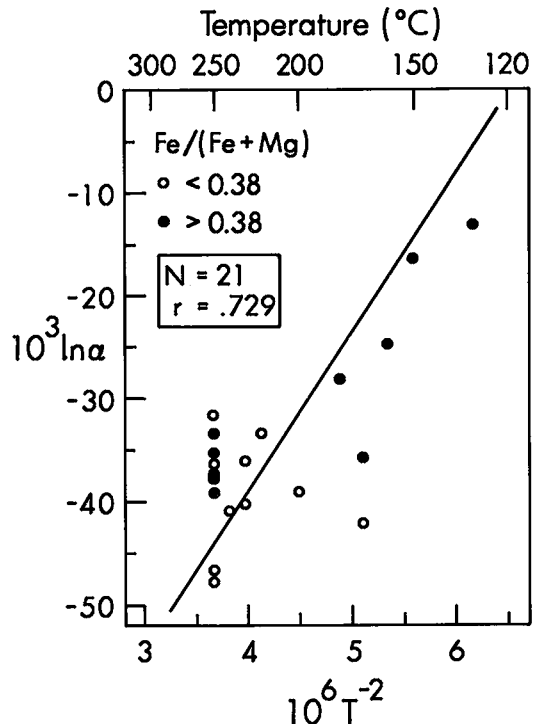


FIG. 6. Chlorite - water hydrogen isotope fractionation data between 130°C and 250°C from the Ohnuma geothermal system, Japan (Marumo *et al.* 1980). The data show a statistically significant positive correlation with $10^6 \cdot T^{-2}$ ($r_{\text{measured}} = 0.729 > r_{\text{crit}} = 0.433$, for 19 degrees of freedom at the 95% confidence level). The positive correlation is unlike all known silicate - water hydrogen isotope fractionation curves (e.g., Taylor 1979), and there is no consistent relationship between $\ln \alpha$ and $\text{Fe}/(\text{Fe} + \text{Mg})$ ratio (data points for $\text{Fe}/(\text{Fe} + \text{Mg}) < \text{and} > 0.38$ are divided equally by the regression line).

(e.g., Taylor 1979). Hence, the mean value of -34.9 is taken as an approximation to the fractionation factor within the 130 – 250°C temperature range. This value is almost identical to that for serpentine – H_2O at 200°C (Wenner & Taylor 1973), suggesting that it is reasonable.

(iv) $\delta^{18}\text{O}$ (chlorite): Wenner & Taylor's (1971) empirical curve is used. Their curve recently has been supported experimentally at 250°C and 300°C by Cole (1985).

(v) $\delta^{18}\text{O}$ (siderite): Becker & Clayton's (1976) data are used.

(vi) $\delta^{18}\text{O}$ (calcite): Friedman & O'Neil's (1977) modification of O'Neil *et al.*'s (1969) original curve is used.

Estimated temperature range for mineralization

The best estimate for the temperature range of hydrothermal processes near the base of the Athabasca sequence is from fluid-inclusion data for the Rabbit Lake deposit and from the Rumble Lake stratigraphic drillhole located near the center of the basin (Fig. 1). Fluid-inclusion studies of quartz and dolomite from Rabbit Lake (which relate to stage II mineralization there), and of overgrowths on clastic quartz grains from the Rumble Lake hole suggest a temperature of ~ 160 – 220°C . Fluid-inclusion data also indicate that the basin was permeated by Na-Ca-Cl brines containing 30 equiv. wt. % NaCl, that this fluid was also involved in mineralization, and that mineralization at Rabbit Lake took place beneath a minimum of ~ 3000 m of sediment (Pagel 1975, 1977, Pagel & Jaffrezic 1977, Pagel *et al.* 1980). These data lend considerable support to the "diagenetic-hydrothermal" hypothesis as they indicate that hydrothermal processes took place at a relatively advanced stage of basin evolution. The latter point has been supported by radiometric dating which indicates that mineralization in several deposits started ~ 100 – 150 Ma after Athabasca sedimentation (e.g., Bray *et al.* 1987). Fluid inclusions were searched for in McClean material but, unfortunately, none were found which would permit a representative study definitely relatable to mineralization. Some support is given to the temperature range of ~ 160 – 220°C , however, from oxygen isotope partition between siderite and chlorite in arsenide/sulfide facies mineralization ($\Delta^{18}\text{O} = 8.7\text{‰}$ from data in Tables 3 and 4) which yields a very approximate temperature of $\sim 180^\circ\text{C}$. Hence, all calculated fluid δD and $\delta^{18}\text{O}$ values have been standardized to 200°C .

In estimating fluid parameters a salt correction has been applied, using Truesdell's (1974) data (quoted in Friedman & O'Neil 1977), only for $\delta^{18}\text{O}$, equivalent data being unavailable for δD . A salt correction is important in this case (-2.2‰) because the fluid-inclusion data suggest that high-salinity brines containing ~ 30 equiv. wt. % NaCl were involved.

FLUID δD – $\delta^{18}\text{O}$ GEOCHEMISTRY (200°C)

Pore fluids in the Athabasca sequence

Calculated fluids in equilibrium with recrystallized illite in sedimentary layers define a tight δD – $\delta^{18}\text{O}$ cluster ($\sim -45\text{‰}$, $\sim +6\text{‰}$) which corresponds closely with the δD and $\delta^{18}\text{O}$ values of a typical modern, evolved formation water such as that in the western Canada sedimentary basin (Fig. 7). The latter fluids are interpreted to be meteoric water – connate sea water mixtures which have undergone variable rock-water oxygen isotope exchange (e.g., Hitchon & Friedman 1969). Although the Athabasca field overlaps a corner of the general primary magmatic-water box (Taylor 1979), there is no additional evidence to consider that magmatic fluids could have been involved (e.g., no intrusions in the McClean deposits, no major intrusions with relevant ages in the basement, only minor mafic dykes elsewhere in the Athabasca basin, and most of these dykes have younger ages: Bray *et al.* 1987).

Possibilities for the origin of the high salinities of the Athabasca pore fluids ($\sim \times 9$ sea water) include dissolution of evaporites, a complete or partial origin as evaporative brines (bitterns), and boiling. The last process can be discounted on the basis of negative fluid-inclusion evidence, *i.e.*, lack of variable gas: liquid ratios (e.g., Pagel 1975, Pagel *et al.* 1980). Evaporation and dissolution of evaporites can be discriminated by the δD – $\delta^{18}\text{O}$ characteristics of the fluids. During the initial stages of sea-water evaporation the light isotopes fractionate preferentially into the vapor phase, as would be expected (Fig. 7). Highly identifiable fluids are produced with positive δD values of up to $\sim +20\text{‰}$, such as those in the Gulf Coast area (Fig. 7; Holser 1979). However, above a salinity of $\sim 14\%$ the effect reverses (Fig. 7) with δD returning to 0‰ at a high salinity of $\sim 40\%$ and a $\delta^{18}\text{O}$ of $\sim +5\text{‰}$. For a salinity of $\sim 30\%$, $\delta\text{D} \cong +5\text{‰}$ and $\delta^{18}\text{O} \cong +6$ – 7‰ , values which do not correspond with the estimated Athabasca pore fluid δD and $\delta^{18}\text{O}$ estimates (Fig. 7). The original Athabasca basin formation-waters, therefore, were probably not bitterns, and the high fluid-inclusion Br/Cl ratios measured by Pagel & Jaffrezic (1977) must have an alternative explanation such as diagenesis of organic matter in shales exposed in the Carswell structure, as discussed by Pagel *et al.* (1980). Hence, the origin of the high salinity of the Athabasca formation-waters seems to have been simply evaporite solution, as can be the case in modern sedimentary basins (e.g., the large zone of evaporite dissolution in the western Canada sedimentary basin; Worsley & Fuzesy 1979). This deduction is reasonable because fluid-inclusion pressure estimates indicate that $> 1,500$ m of sediment which could have contained evaporites have been erosionally removed, the topmost Carswell Formation consists of > 500 m

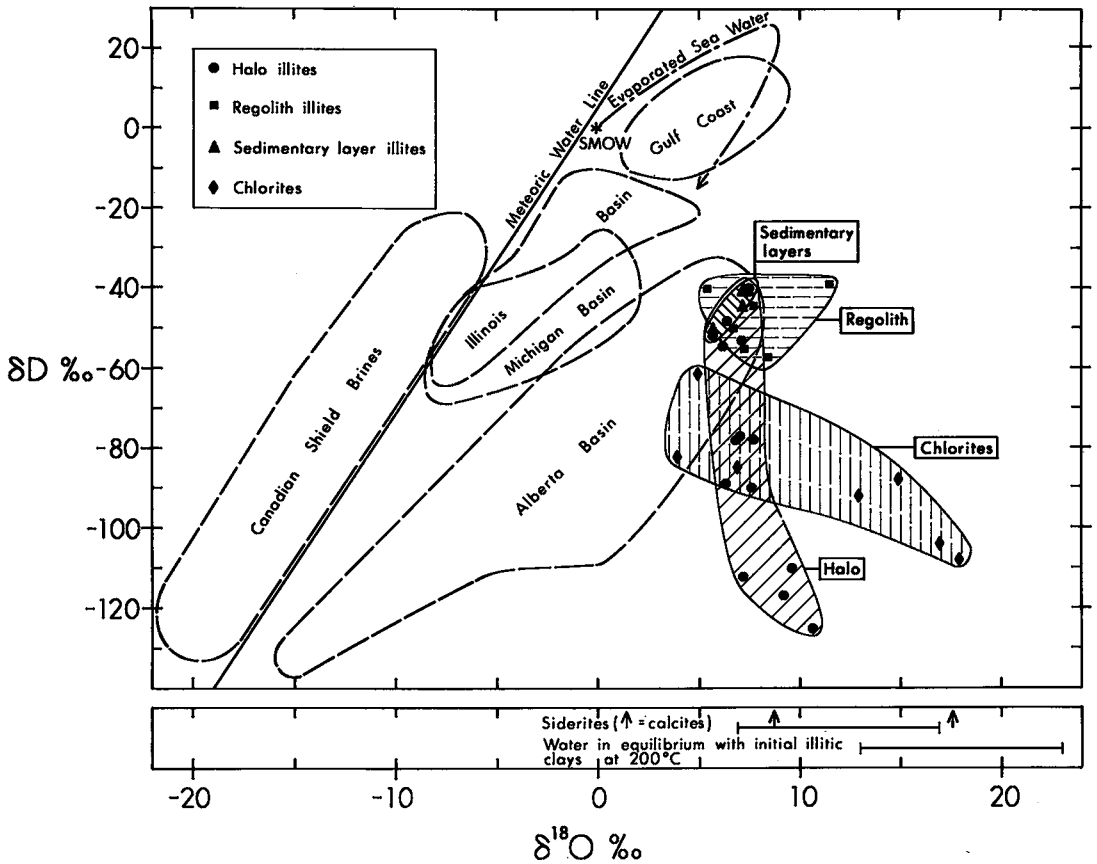


FIG. 7. Estimated fluid δD and $\delta^{18}O$ values for original pore fluids in the Athabasca sequence (from recrystallised sedimentary layers), fluids which interacted with basement away from mineralization (from "regolith"), fluids which were involved in the hydrothermal alteration halo and in "bleached"-facies mineralization, fluids which were involved in chloritic arsenide- and sulfide-facies mineralization, and fluids which were in equilibrium with carbonate within and below mineralization. The latter fluid-isotope estimates are compared with fluid-isotope values for meteoric water, formation-waters from the Alberta, Michigan, Illinois and Gulf Coast Basins (from Taylor 1979), evaporated sea waters (Holser 1979), Canadian Shield brines (Frape & Fritz 1982), and fluids in equilibrium with basement graphitic semi-pelites, initially illitic clays, under rock \gg water-dominated conditions at 200°C (see text).

of algal laminites and oolitic and stromatolitic dolostones with evaporite pseudomorphs and evaporite solution-collapse breccias (Hendry & Wheatley 1985), and palaeomagnetic data indicate that N. Saskatchewan was equatorially located in the relevant time interval. Regarding the last point, palaeomagnetic reconstructions (Irving 1979) indicate that, between deposition of the Manitou Falls Formation which immediately overlies the host Wolverine Point Formation (1430 ± 30 Ma; Armstrong & Ramaekers 1985) and the start of uranium mineralization (at ~ 1350 – 1300 Ma; e.g., Bray *et al.* 1987), the Athabasca Basin was within 30° of the equator. In fact, at 1400 Ma, the Basin was only 5° from the equator, and at 1350 Ma was on the equator. The δD and $\delta^{18}O$ data also indicate that the Athabasca pore fluids were not Canadian Shield brines (Frape

& Fritz 1982); the latter are characterized by δD – $\delta^{18}O$ values above the meteoric water line (Fig. 7).

An implication of the origin of high fluid salinity by evaporite dissolution is that the high-density brines would have sunk gravitationally to occupy the bottom of the sedimentary basin. This process has recently been documented in the Salton Sea geothermal system, California (Williams & McKibben 1987) where a deep, hot (up to $360^\circ C$), saline (19–26 wt. % TDS) brine formed by evaporite dissolution is separated from an overlying less saline ($< 10\%$ TDS) brine by a sharp, density-controlled interface.

Fluids which interacted with basement away from mineralization

Fluids which interacted with basement over the

same age range as that for formation of diagenetic interstitial illite (see above; Bray *et al.* 1987) have similar calculated δD and $\delta^{18}O$ values to those estimated for the original Athabasca pore fluids (Fig. 7). Hence, the fluid which produced altered basement in its final form either from a weathered "regolith", or an unweathered precursor, was isotopically the same as the Athabasca formation-water. In the McClean area, basement alteration typically penetrates ~20–100 m (Wallis *et al.* 1983, 1984), and alteration at Cigar increases in thickness under mineralization to ~100 m (Fouques *et al.* 1986).

Fluids involved in hydrothermal alteration and "bleached" facies mineralization

Fluids in equilibrium with illite from the hydrothermal alteration halo around mineralization and from "bleached" facies mineralization show a very distinctive elongate $\delta D - \delta^{18}O$ field (Fig. 7). The range of $\delta^{18}O$ values (~ +5‰ to +10‰) is constant and is basically the same as that calculated for Athabasca formation-waters. In contrast, the hydrogen-isotope ratios define a large range of ~90‰, extending from δD values coincident with those of Athabasca formation-waters (~

-35‰ to ~-60‰) to values as low as ~ -125‰ (Bray *et al.* 1984). There is a slight association between the lowest δD values and higher $\delta^{18}O$ values.

The δD variation also shows a very close relationship with uranium mineralization. In the plans and sections of the North and South Zone pods in Figure 8 it can be seen that all illite δD values (measured) $\geq -79‰$ ($n = 5$) either lie to the side of (180, 2076) or above (1208, 2065, 2071, 2076) the 0.5% U_3O_8 -ft grade \times thickness cut-off contour, whereas all illite δD values (measured) $\leq -102‰$ ($n = 9$) lie within mineralization. Samples with the lowest δD values such as 2058 (-135‰), 2038 (-137‰), 1136 (-142‰) and 2019 (-150‰) lie close to or within the highest grade mineralization. This relationship also can be seen in a graph of illite δD (measured) versus % U_3O_8 for the assayed 1–2 ft. lengths of half-core which contain the analyzed illite samples (Fig. 9). The plot shows particularly well that there is a δD gap between ~ -80‰ and ~ -100‰ (measured) which corresponds to the difference between zero and weak mineralization (> ~0.05% U_3O_8).

Hence, it is apparent that the hydrogen, but not

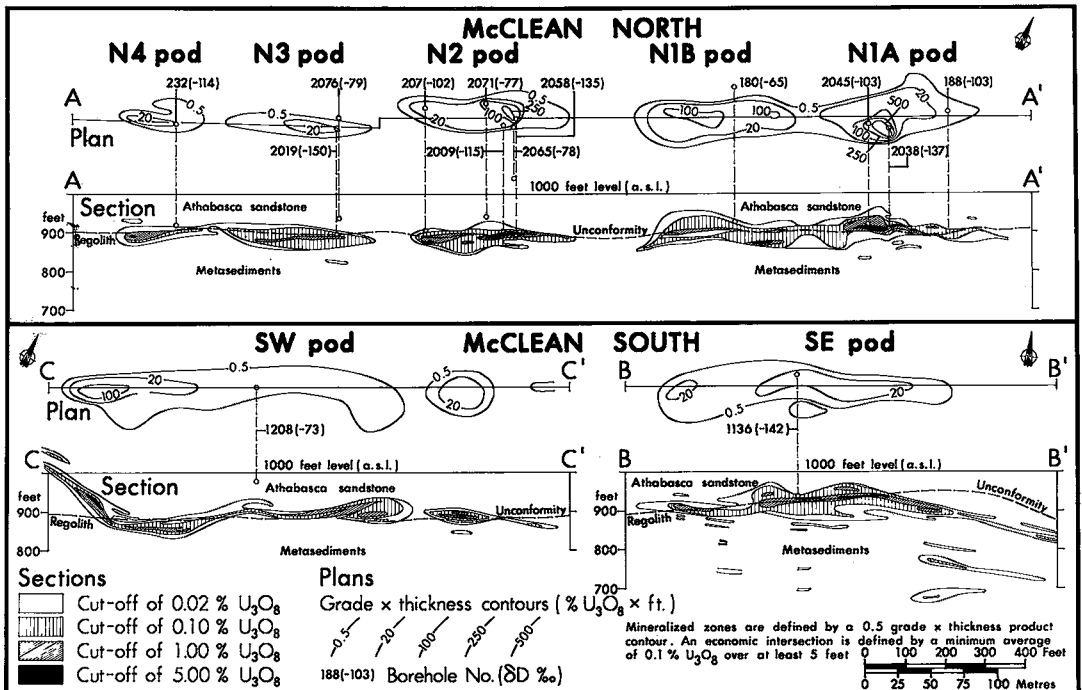


FIG. 8. Contoured plans and sections of the McClean mineralized pods. Illite from hydrothermal alteration and "bleached"-facies mineralization with δD values (measured) $\geq -79‰$ ($n = 5$) lies outside mineralization, either to the side or above, whereas illite with δD values (measured) $\leq -102‰$ ($n = 9$) lies within mineralization. Samples with the lowest δD values (-150‰ to -135‰) lie close to or within the highest grade mineralization. (Drafted from Canadian Occidental Petroleum Ltd. / INCO Metals Co. long sections).

the oxygen-isotope compositions of the fluids associated with the hydrothermal alteration halo and "bleached" facies mineralization were modified selectively in direct association with uranium mineralization. An explanation for the low δD values must take into account two other observations: (1) the graphite depletion/modification observed beneath the ore zone, and (2) the negative $\delta^{13}C$ values for ore-zone carbonate (-13.2‰ to -1.7‰ ; $n = 14$) related to more negative basement graphite (-25.6‰ to -19.6‰ , $n = 6$; Bray *et al.* 1982) which establish an isotopic connection with processes within the basement. Hence, we suggest (Bray *et al.* 1984) that the fluid δD values were changed selectively by interaction with isotopically light hydrogen contained in $CH_4 \pm H_2S \pm H_2$ derived by interaction with basement graphitic metasediment (e.g., Taylor 1979, who pointed out this possibility). At $200^\circ C$ CH_4 is 68‰ lighter than H_2O (Fig. 10; Friedman & O'Neil 1977). For Athabasca formation-water with $\delta D \sim -50\text{‰}$, the δD of CH_4 in equilibrium would have been $\sim -120\text{‰}$. Upward movement of the CH_4 and oxidation to H_2O and CO_2 , evident also from the low carbonate $\delta^{13}C$ values of -13.2‰ to 1.7‰ , would have selectively lowered the δD value of the formation-water. Interestingly, the lowest calculated "bleached" facies δD value of $\sim -125\text{‰}$ corresponds

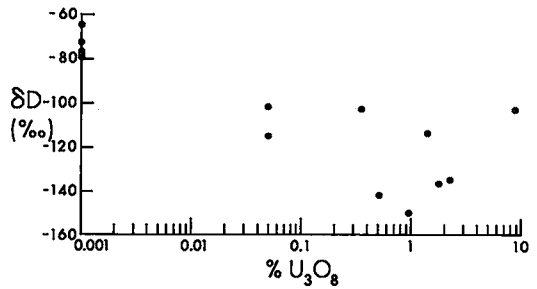


FIG. 9. Illite δD (measured) plotted against $\% U_3O_8$ for the assayed 1–2 ft lengths of half-core which contain the analyzed illite samples. Note that samples with less-negative δD values ($\geq -79\text{‰}$; $n = 5$) contain no uranium, whereas samples with $\delta D \leq -102\text{‰}$ ($n = 9$) contain $>0.05\%$ U_3O_8 , and up to $\sim 9\%$ U_3O_8 .

to the maximum depletion which CH_4 could have produced. This process would have been enhanced by any H_2S produced and oxidized: both dissolved and gaseous H_2S are hydrogen-isotopically depleted relative to liquid H_2O in isotopic equilibrium, at all temperatures (Fig. 10; Neuburg *et al.* 1977). For example, at $200^\circ C$, $\delta D(H_2O.l) - \delta D(H_2S.l) = 508\text{‰}$ and $\delta D(H_2O.l) - \delta D(H_2S.g) = 492\text{‰}$

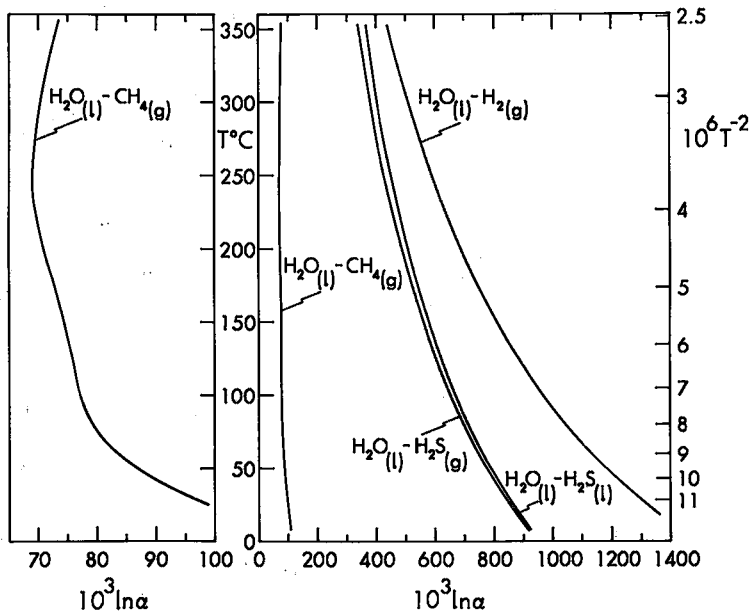


FIG. 10. Hydrogen isotope fractionations between $H_2O(l)$ and $CH_4(g)$ (calculated from Friedman & O'Neil 1977), $H_2S(g)/H_2S(l)$ (latter two from Neuburg *et al.* 1977) and $H_2(g)$ (calculated from Friedman & O'Neil 1977; same format as Friedman & O'Neil 1977). The irregular shape of the $\delta D(H_2O.l) - \delta D(CH_4.g)$ curve is a consequence of combining the $\delta D(H_2O.l) - \delta D(H_2O.g)$ and $\delta D(H_2O.g) - \delta D(CH_4.g)$ curves.

(Fig. 10; $\delta D(H_2S.l)$ refers to H_2S dissolved in liquid H_2O). Additional depletion also would have resulted from oxidation of H_2 because at $200^\circ C$ H_2 is very much lighter, by $\sim 700\%$, than H_2O

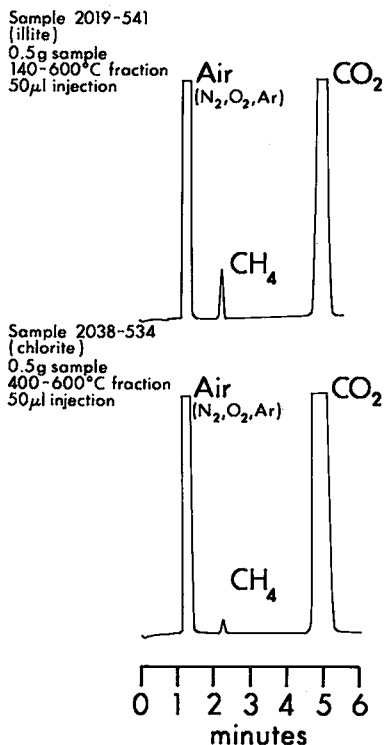


FIG. 11. Gas chromatograms of carbon gas species released by heating samples of deuterium-depleted "bleached"-facies illite (sample 2019-541 in the N3 pod; $\delta D = -150\%$; Fig. 5) and chloritic material in arsenide/sulfide facies (sample 2038-534 from the N1A pod; Fig. 5). The traces, which are representative of a further 15 samples, show well-defined "air" (N_2 , O_2 , Ar), CH_4 and CO_2 peaks. Retention times and peak areas have been calibrated using gas mixtures of known composition. The corrected CO_2/CH_4 ratios are 28 v/v (2019-541) and 652 v/v (2038-534) suggesting that CO_2 was the principal carbon gas species present. The "air" peak is not all from the sample because "air" was introduced during sample injection in the simple experimental technique used. CO_2 and CH_4 from air were not detected, as determined by blank runs. The 0.5 g samples were degassed for at least 30 min. at $140^\circ C$, and the gas removed prior to degassing at higher temperatures. Analyses, on $50 \mu l$ samples withdrawn by syringe from a heated silica glass tube, were carried out on a Hewlett Packard HP 5890 gas chromatograph using a $1/8" \times 10'$ column of Porapak Q (100/120 mesh) at $30^\circ C$. Carrier gas: helium. Injector temperature: $120^\circ C$. Detector type: TCD. Detector temperature: $120^\circ C$. Flow rates: $19.5 \text{ cm}^3/\text{min}$ (column) and $50.0 \text{ cm}^3/\text{min}$ (reference).

(Fig. 10; Friedman & O'Neil 1977). $CO_2 \pm CH_4 \pm H_2S \pm H_2$ may have formed a physically separate gas phase: their solubilities in saline brines are not very high because of the salting-out effect. For example, at $200^\circ C$ and 700 bar (Pagel *et al.* 1980) the solubilities of CH_4 and CO_2 in $\sim 30 \text{ wt.}\%$ NaCl solution are $\sim 1,300 \text{ ppm}$ (McGee *et al.* 1981) and $\sim 30,000 \text{ ppm}$ (Takenouchi & Kennedy 1965), respectively. The existence of CO_2 , CH_4 and S species is shown by gas chromatographic analysis of gases released by heating (140–600°C fraction) illitic sheet silicates associated with "bleached" facies mineralization and chloritic material from the arsenide/ sulfide facies (see Fig. 11, and caption for analytical methods). CO_2 and CH_4 were detected as well-defined peaks (Fig. 11), and the presence of S species was evident from a deposit of sulfur in the glass degassing tube as well as gas-chromatographic detection of H_2S and SO_2 at longer retention times. The original form of the S species is unknown because of high-temperature reactions during degassing. CO_2/CH_4 ratios of 28 and 652 (Fig. 11) suggest that CO_2 was the dominant carbon gas species present.

Generation of buoyant vapor bubbles could have considerably enhanced geochemical transfer of gaseous species from the basement to the overlying sandstone, which otherwise might not have occurred very readily from small fractures, and would have efficiently supplied reductant for the precipitation of U^{IV} oxides. CO_2 in a separate gas phase could have caused a positive $\delta^{18}O$ shift in the overlying Athabasca formation-water since, at $200^\circ C$, it is $\sim 26\%$ heavier than H_2O in equilibrium (Friedman & O'Neil 1977). However, the effect would not have been large because the CO_2 would have been continuously in contact with and exchanging with the overlying formation-water. The effect, if any, was small because of the general lack of an observed positive $\delta^{18}O$ shift. However, the effect might explain the slightly higher $\delta^{18}O$ values of the lowest δD fluids (see below for an alternative explanation).

In conclusion, upward mass-transfer of $CO_2 \pm CH_4 \pm H_2S \pm H_2$ can explain the closeness of the relationship between δD and uranium mineralization because $CH_4 \pm H_2S \pm H_2$ would have been, simultaneously, the source of the isotopically light hydrogen and the reductant to precipitate U^{VI} in solution as U^{IV} oxides. The process might also explain an unusual statistically significant relationship observed between illite δD values (measured), and $^{40}Ar/^{39}Ar$ and K/Ar ages (11 pairs, Fig. 12). The most depleted δD values correlate with the youngest ages, as well as with the higher U_3O_8 grades (Fig. 9), a relationship which can be interpreted as a consequence of longer periods of $CH_4 \pm H_2S \pm H_2$ (reductant) supply which caused lower δD 's, younger ages, and more concentrated U mineralization.

Fluids involved in arsenide/sulfide facies mineralization (δD and $\delta^{18}O$ from chlorites)

Calculated fluids in equilibrium with chlorite from arsenide/sulfide facies mineralized sandstones show an inclined $\delta D - \delta^{18}O$ distribution different from that of alteration halo/"bleached" facies mineralization fluids (Fig. 7). The range of δD values ($\sim -70\%$ to $\sim -115\%$) corresponds satisfactorily with that of the more negative halo/"bleached" facies fluids which are associated with $> 0.05\%$ U_3O_8 mineralization, and is also interpreted to be a result of interaction with hydrogen-isotopically-light $CH_4 \pm H_2S \pm H_2$, CO_2 , CH_4 and S species also have been detected gas-chromatographically by heating chloritic material (Fig. 11). The fluid $\delta^{18}O$ values, on the other hand, range from values estimated to be typical of the original Athabasca formation-waters and alteration halo/"bleached" facies, to values shifted positively as high as $\sim +18\%$. Hence, the fluids of the arsenide/sulfide facies mineralization may have been concomitantly enriched in ^{18}O and depleted in deuterium (Fig. 7). Carbon and sulfur isotope data clearly indicate geochemical linkage between basement processes and mineralization (Bray *et al.* 1982), and arsenide/sulfide facies mineralization occurs in basement as much as 17 m below the unconformity (Wallis *et al.* 1984). Hence, the fluid $\delta^{18}O$ shift is interpreted to be a result of formation- H_2O - basement interaction. Sedimentary clays, the precursors to the basement graphitic semi-pelites, have $\delta^{18}O$ values typically between $\sim +15\%$ and $\sim +25\%$ (e.g., Hoefs 1980). The salt-corrected illite - water $\delta^{18}O$ fractionation at $200^\circ C$ is $\sim +4\%$, and thus fluids in equilibrium with basement under rock-dominated conditions would have had $\delta^{18}O$ values of $\sim +11\%$ to $\sim +21\%$ (Fig. 7), a range which corresponds closely to that of the $\delta^{18}O$ enriched fluids in equilibrium with chlorite ($\sim +13\%$ to $\sim +18\%$). The cause of fluid flow out of the basement into the overlying sediments is not known. However, two-phase flow induced by upward vapor-bubble migration would clearly have been an effective mechanism. Mixing with such an ^{18}O -enriched fluid could also have produced the slightly higher $\delta^{18}O$ values of the lowest δD halo/"bleached" facies fluids (Fig. 7; see above).

The inclined $\delta D - \delta^{18}O$ trend shown by the fluids in equilibrium with the chlorites is interpreted to indicate that the zone of arsenide/sulfide mineralization was the site of *mixing* between formation-waters (oxidized) and fluids which had interacted with basement (reduced). Hence, the isotope data show a definite correlation between the interpreted zone of potential redox reactions and U^{IV} precipitation. The "bleached" facies of mineralization and the halo were above the main fluid-mixing zone.

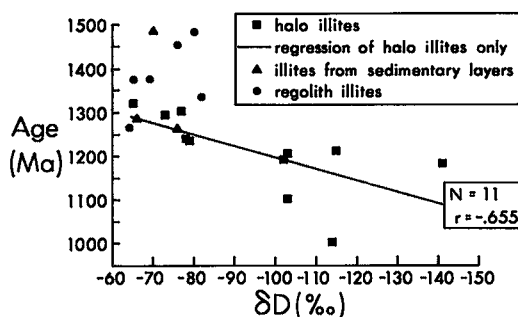


FIG. 12. Relations between illite laser-probe $^{40}Ar/^{39}Ar$ and conventional K-Ar ages (Bray *et al.* 1987) and measured δD values for illites from recrystallized sedimentary layers, altered basement away from mineralization ("regolith"), and the hydrothermal alteration halo and "bleached" mineralization facies. The age versus halo/"bleached"-facies illite δD data show a statistically significant negative correlation ($r_{measured} = -0.655 < r_{crit} = -0.602$ for 9 degrees of freedom at the 95% confidence level). The sedimentary layer and "regolith" illites show a range from ages appropriate to their relatively less negative δD values to older ages. These relationships suggest that measured δD values of $\sim -80\%$ to -60% reflect formation-waters, whereas the more negative values ($\leq -102\%$, and down to -142% in this diagram) reflect deuterium depletion.

Fluids in and below arsenide/sulfide facies mineralization ($\delta^{18}O$ from carbonates)

Siderite is a major component of arsenide/sulfide facies mineralization as can be seen from the CO_2 contents (Table 4) which average 6.6 ± 4.4 wt. % CO_2 ($n = 8$). The siderite occurs as $\sim 500 \mu m$ particles scattered throughout the chlorite-illite matrix which surrounds embayed quartz grains (Wallis *et al.* 1984). The calculated $\delta^{18}O$ values of fluids in equilibrium with this disseminated carbonate show exactly the same range of $\delta^{18}O$ values as that calculated from coexisting chlorite (Fig. 7), a reflection of the fact that the average carbonate-chlorite $\delta^{18}O$ fractionation gives a reasonable temperature of $\sim 180^\circ C$ (see above). This correspondence is satisfactory because it confirms the positive $\delta^{18}O$ shift deduced from chlorites associated with the arsenide/sulfide facies mineralization.

The $\delta^{18}O$ values of fluids in equilibrium with carbonate in veins below mineralization are exactly the same as those for disseminated carbonate (and chlorite; Fig. 7). Five of the eight values were derived from veins well within basement, specifically 9 m, 12 m, 13 m, 20 m and 22 m below the unconformity. This similarity indicates that a fluid with the $\delta^{18}O$ values inferred for that involved in arsenide/sulfide facies uranium mineralization did evolve in the basement. Hence, basement - fluid interaction is supported as a mechanism for generating the positive

$\delta^{18}\text{O}$ shifts. Four of the five samples from veins in basement give $\delta^{18}\text{O}$ values at the high end of the total range (+21.4‰ to +25.1‰, measured, *cf.* +15.2‰ to +25.2‰ for disseminated carbonate; Table 4), as would be expected. Also, the $\delta^{13}\text{C}$ values for vein carbonate from below and within arsenide/sulfide facies mineralization are the same (Bray *et al.* 1982), adding further support.

Reasons against meteoric water exchange

It has been suggested that the low δD values of illite were produced by later exchange with meteoric waters with δD values comparable to those of modern meteoric water in the Athabasca basin (Wilson *et al.* 1987). The two strongest items of evidence against this interpretation are:

(i) As shown clearly in Figure 8, δD depleted illite samples are enclosed in an envelope of undepleted material both to the side and above. Wilson *et al.* (1987) demonstrated for the Key Lake deposit that illite from the proximity of the ore zone cannot be differentiated (crystallographically) from other illite. Hence, the interpretation of meteoric-water exchange suggests that water passed through some illite without exchange in order to react with some other identical illite, an unlikely possibility.

(ii) In the McClean deposits D-depleted illite and chlorite samples are intimately intergrown with U oxides which are highly reactive with medium-high Eh groundwater of meteoric origin. The deposits are contained in hematite-bearing, diagenetically altered Athabasca sandstone containing no minerals to reduce the Eh of meteoric groundwaters. How then could recent meteoric waters have exchanged with illite and chlorite without reacting with the primary U oxides?

The above arguments are supported by four additional points:

(i) Figure 6 of Wilson *et al.* (1987) clearly shows an interesting observation: not only is the interlamellar H_2O D-depleted, but the hydroxyl H_2O is also depleted. Hence, Wilson *et al.* (1987) are suggesting that the isotopic modification of hydroxyl H has occurred without reactive crystallographic change of the illite from a high-grade diagenetic/low-grade metamorphic 3T polytype to a low-temperature 1M polytype. This lack of change is unlikely considering that Bray *et al.*'s (1987) work has shown that the illite has not been reheated above $\sim 140^\circ\text{C}$.

(ii) The youngest McClean illite sample not within ~ 2 mm of a U mineral nodule (Bray *et al.* 1987) has an age of 1002 ± 33 Ma (Fig. 12). Hence, the meteoric-water exchange interpretation suggests modification of hydroxyl as well as interlamellar H, the latter being in sites similar to those of K, without complete liberation of uncharged radiogenic Ar; this is another unlikely possibility.

(iii) D depletion of the illite samples is supported

by D depletion of chlorite samples. For example, the δD values of fluids calculated to be in equilibrium, as shown in Figure 7, show significant overlap. Hence, the interpretation of meteoric-water exchange also suggests D exchange with chlorites, unaccompanied by reaction either of the chlorite or the intergrown U oxides.

(iv) The clearest discriminatory test between the two interpretations would be to determine the δD values of primary fluid inclusions relating to U mineral deposition. Pagel *et al.* (1980) present 9 δD determinations for fluid inclusions in their stage II dolomite-bearing samples from the Rabbit Lake deposit which define a 31‰ range from -94 ‰ to -63 ‰. Reference to Figure 7 shows that values of -94 ‰, -87 ‰ and -79 ‰ are well within the calculated illite and chlorite D-depleted fluid fields. Hence, Pagel *et al.*'s (1980) determinations demonstrate the occurrence of D-depleted, high-temperature fluids (homogenization temperatures = < trapping temperatures ranging from 119.5 – 144.7°C) during mineralization.

SUMMARY OF PRINCIPAL CONCLUSIONS

1. The estimated δD and $\delta^{18}\text{O}$ values of the original Athabasca sequence pore fluid (~ -45 ‰, $\sim +6$ ‰) are similar to those of some evolved, modern formation-waters.

2. The high salinity (~ 30 equiv. wt. % NaCl) of the Athabasca formation-water was produced by evaporite dissolution, a deduction which corresponds with the fact that the upper part of the Athabasca sequence (Carswell formation) contains evaporite solution-collapse breccias (Hendry & Wheatley 1985). The fluids were not bitterns or equivalent to modern Canadian Shield brines. An implication of the origin the high fluid salinity by evaporite dissolution is that the high-density brines would have sunk gravitationally to the bottom of the sedimentary basin, a process which has recently been documented from the Salton Sea geothermal system, California (Williams & McKibben 1987).

3. The δD and $\delta^{18}\text{O}$ values of the fluids recorded by altered basement "regolith" are not those of meteoric waters which would have been involved in chemical weathering, but are similar to those inferred for the original Athabasca formation-water. Hence, altered basement either completely re-equilibrated isotopically with the formation-water, or was produced directly by formation-water/basement interaction.

4. The "diagenetic-hydrothermal" hypothesis for the origin of Canadian unconformity-related uranium mineralization (Hoeve & Sibbald 1978, Hoeve *et al.* 1980, Sibbald *et al.* 1981) is strongly supported by isotopic evidence for formation-water/basement

interaction and generation of reductant: (i) $\delta^{18}\text{O}$ values of the fluids involved in the hydrothermal alteration halo and in "bleached"-facies mineralization are the same as those calculated for the original Athabasca formation-water ($\sim +5\%$ to $\sim +10\%$); (ii) δD depletion of fluids from the alteration-halo/"bleached" facies of mineralization to values as low as $\sim -125\%$ can be interpreted as a result of selective modification by hydrogen-isotopically-light $\text{CH}_4 \pm \text{H}_2\text{S} \pm \text{H}_2$ derived by interaction with basement graphitic metasediments; (iii) δD depletion of fluids from the alteration-halo/"bleached" facies of mineralization correlates with higher U_3O_8 grades and with younger laser-probe $^{40}\text{Ar}/^{39}\text{Ar}$ and conventional K/Ar ages; (iv) calculated arsenide/sulfide-facies mineralization fluids show not only a marked positive $\delta^{18}\text{O}$ shift from Athabasca formation-water values to values as high as $\sim +18\%$ (calculated from both chlorites and carbonates), but also D depletion; the former trend is interpreted to be a result of formation-water - basement interaction; (v) $\delta^{18}\text{O}$ values of carbonate from veins beneath mineralization (9-22m below the unconformity) show that a fluid high in ^{18}O did indeed evolve in fractured basement. A diagrammatic summary of the fluid processes and their isotopic effects is given in Figure 13.

5. The loci of chloritic arsenide/sulfide-facies uranium mineralization were mixing zones (Fig. 13) between oxidized formation-waters and reduced fluids which had interacted with basement (reduced) as shown by $\delta\text{D} - \delta^{18}\text{O}$ covariation. Hence, the isotope data specifically show a correlation between interpreted zones of redox reactions and U^{IV} oxide precipitation.

6. The presence of CO_2 , CH_4 and S species has been confirmed by gas chromatographic analysis of gases released by heating (140-600°C fraction) both illitic sheet silicates associated with "bleached"-facies mineralization and chloritic material from arsenide/sulfide-facies mineralization. CO_2/CH_4 ratios of 28 and 652 for the two examples given suggest that CO_2 was the dominant carbon gas species.

7. $\text{CO}_2 \pm \text{CH}_4 \pm \text{H}_2\text{S} \pm \text{H}_2$ may have formed a physically separate gas phase: the solubilities of CH_4 and CO_2 are not very high in saline solutions ($\sim 1,300$ ppm and $\sim 30,000$ ppm, respectively). Such a buoyant gas phase would have acted as an efficient reductant.

ACKNOWLEDGEMENTS

This research was financially and logistically supported by the Canadian Occidental Petroleum Ltd.

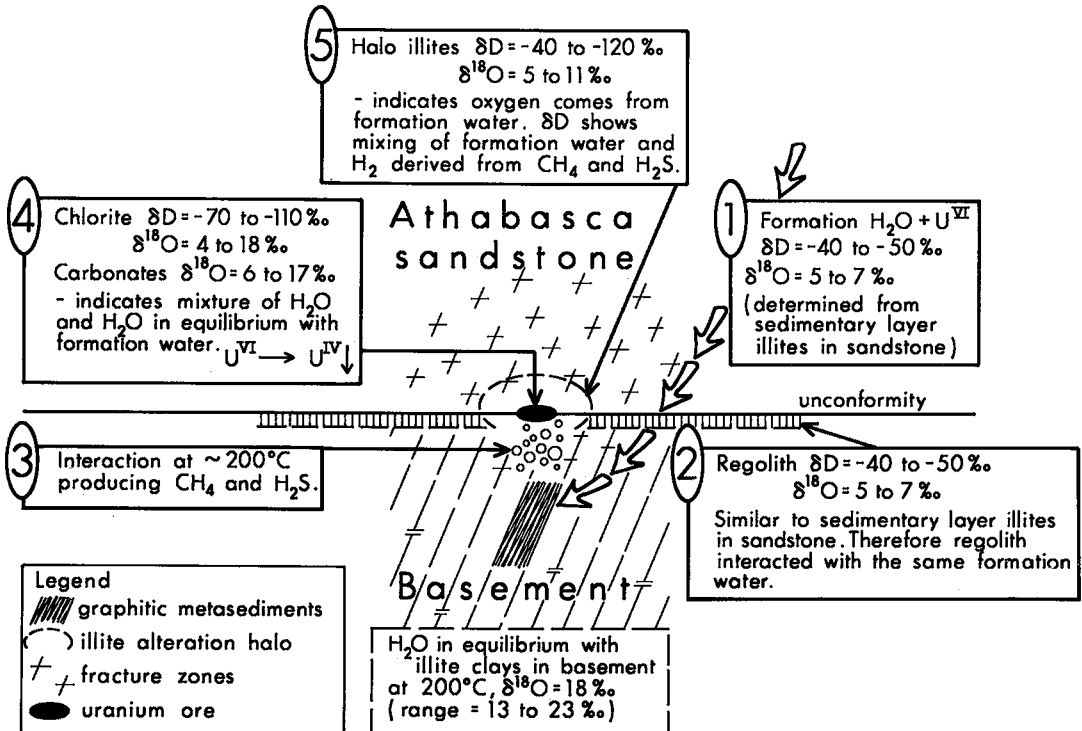


FIG. 13. Diagrammatic summary of estimated fluid δD and $\delta^{18}\text{O}$ values, and interpretations.

(Minerals Division)/INCO Metals Co. joint venture-ship which discovered the McClean group of uranium deposits. Receipt of this research grant is acknowledged with very considerable appreciation. Accordingly, we particularly thank Dr. J.J. Brummer, Dr. R.H. Wallis, Dr. J.P. Golightly, Mr. N. Saracoglu and other Canadian Occidental Petroleum Ltd. (Minerals Division) and INCO Metals Co. personnel for unstinting assistance and encouragement. F.J.L. acknowledges receipt of grants from the Natural Sciences and Engineering Research Council of Canada for supporting his isotope analytical facilities and particularly thanks Diane Caird for technical assistance. C.J.B. and E.T.C.S. acknowledge receipt of Natural Sciences and Engineering Research Council of Canada grant E5788 (to E.T.C.S.) for purchase of a gas chromatograph. We also thank Krueger Enterprises Inc. (Dr. H.W. Krueger), the Isotope Lab. at the University of Waterloo, and Dr. H.R. Krouse (University of Calgary) for analytical assistance, and Subhash Shanbhag (draftsman), Brian O'Donovan (photographer), Gita Cheryan and Sonia Hopwood (secretaries) for their great help, which we much appreciate.

REFERENCES

- ARMSTRONG, R.L. & RAMAEKERS, P. (1985): Sr isotopic study of Helikian sediment and diabase dikes in the Athabasca Basin, northern Saskatchewan. *Can. J. Earth Sci.* **22**, 399-407.
- BECKER, R.H. & CLAYTON, R.N. (1976): Oxygen isotope study of a Precambrian banded iron-formation, Hammersley Range, Western Australia. *Geochim. Cosmochim. Acta* **40**, 1153-1165.
- BRAY, C.J., SPOONER, E.T.C., GOLIGHTLY, J.P. & SARACOGLU, N. (1982): Carbon and sulphur isotope geochemistry of unconformity-related uranium mineralization, McClean Lake deposits, N. Saskatchewan, Canada. *Geol. Soc. Amer., Ann. Meet. Abstr. Programs* **14**, No. 7, 451.
- _____, _____, HALL, C.M., YORK, D., BILLS, T.M. & KRUEGER, H.W. (1987): Laser probe $^{40}\text{Ar}/^{39}\text{Ar}$ and conventional K/Ar dating of illites associated with the McClean unconformity related uranium deposits, N. Saskatchewan, Canada. *Can. J. Earth Sci.* **24**, 10-23.
- _____, _____ & LONGSTAFFE, F.J. (1984): Oxygen and hydrogen isotope geochemistry of unconformity-related uranium mineralization, McClean deposits, N. Saskatchewan, Canada. *Geol. Assoc. Can./Mineral. Assoc. Can. Ann. Meet., Programs Abstr.* **9**, 48.
- COLE, D.R. (1985): A preliminary evaluation of oxygen isotope exchange between chlorite and water. *Geol. Soc. Amer. Ann. Meet., Abstr. Programs* **17**, No. 7, 550.
- DAHLKAMP, F.G. (1978): Geological appraisal of the Key Lake U-Ni deposits, northern Saskatchewan. *Econ. Geol.* **73**, 1430-1449.
- ESLINGER, E.V. & SAVIN, S.M. (1973): Mineralogy and oxygen isotope geochemistry of the hydrothermally altered rocks of the Ohaki-Broadlands, New Zealand geothermal area. *Amer. J. Sci.* **273**, 240-267.
- FOGWILL, W.D. (1985): Canadian and Saskatchewan uranium deposits: compilation, metallogeny, models, exploration. In *Geology of Uranium Deposits* (T.I.I. Sibbald & W. Petruk, eds.). *Can. Inst. Mining Metall. Spec. Vol.* **32**, 3-19.
- FOUQUES, J.P., FOWLER, M., KNIPPING, H.D. & SCHIMANN, K. (1986): Le gisement d'uranium de Cigar Lake: découverte et caractéristiques générales. *Can. Inst. Mining Metall. Bull.* **79**, 70-82.
- FRAPE, S.K. & FRITZ, P. (1982): The chemistry and isotopic composition of saline groundwaters from the Sudbury basin, Ontario. *Can. J. Earth Sci.* **19**, 645-661.
- FRIEDMAN, I. & O'NEIL, J.R. (1977): Compilation of stable isotope fractionation factors of geochemical interest. *U.S. Geol. Survey Prof. Paper* **440-KK**.
- HENDRY, H.E. & WHEATLEY, K.L. (1985): The Carswell Formation, northern Saskatchewan: stratigraphy, sedimentology, and structure. *Geol. Assoc. Can. Spec. Pap.* **29**, 87-103.
- HITCHON, B. & FRIEDMAN, I. (1969): Geochemistry and origin of formation waters in the western Canada sedimentary basin - I. Stable isotopes of hydrogen and oxygen. *Geochim. Cosmochim. Acta* **33**, 1321-1349.
- HOEFS, J. (1980): *Stable Isotope Geochemistry*. Springer-Verlag, Berlin-Heidelberg-New York.
- HOEVE, J. & SIBBALD, T.I.I. (1978): On the genesis of Rabbit Lake and other unconformity type uranium deposits in northern Saskatchewan, Canada. *Econ. Geol.* **73**, 1450-1473.
- _____, _____, RAMAEKERS, P. & LEWRY, J.F. (1980): Athabasca Basin unconformity-type uranium deposits: a special class of sandstone-type deposits? In *Uranium in the Pine Creek Geosyncline*, Proc. Symposium, Vienna, Int. Atomic Energy Agency, 575-594.
- HOLSER, W.T. (1979): Trace elements and isotopes in evaporites. In *Marine minerals* (R.G. Burns, ed.). *Mineral. Soc. Amer., Reviews in Mineralogy* **6**, 295-346.
- IRVING, E. (1979): Paleopoles and paleolatitudes of

- North America and speculations about displaced terranes. *Can. J. Earth Sci.* 16, 669-694.
- MACDONALD, C. (1985): Mineralogy and geochemistry of the sub-Athabasca regolith near Wollaston Lake. In *Geology of Uranium deposits* (T.I.I. Sibbald & W. Petruk, eds.). *Can. Inst. Mining Metall. Spec. Vol. 32*, 155-158.
- MARUMO, K., NAGASAWA, K. & KURODA, Y. (1980): Mineralogy and hydrogen isotope geochemistry of clay minerals in the Ohnuma geothermal area, north-eastern Japan. *Earth Planet. Sci. Lett.* 47, 255-262.
- MCGEE, K.A., SUSAK, N.J., SUTTON, A.J. & HAAS, J.L., JR. (1981): The solubility of methane in sodium chloride brines. *U.S. Geol. Surv. Open-file Rep.* 81-1294.
- MINING ANNUAL, REVIEW (1984): *Uranium*. London, Mining Journal Ltd., 85-87.
- MINING ANNUAL REVIEW (1985): *Uranium*. London, Mining Journal Ltd., 109-110.
- MINING ANNUAL REVIEW (1985): *Canada, Uranium*. London, Mining Journal Ltd., 312-315.
- NEUBURG, H.J., ATHERLEY, J.F. & WALKER, L.G. (1977): Girdler-sulfide process physical properties. *Atomic Energy of Canada Ltd., Rep. AECL-5072*.
- NUKEM MARKET REPORT (1986): Uranium production of the Western World. *NUKEM Market Report 1*, 10.
- O'NEIL, J.R., CLAYTON, R.N. & MAYEDA, T.K. (1969): Oxygen isotope fractionation in divalent metal carbonates. *J. Chem. Physics* 51, 5547-5558.
- PAGEL, M. (1975): Détermination des conditions physico-chimiques de la silicification diagenétique des grès Athabasca (Canada) au moyen des inclusions fluides. *Compte Rendu Acad. Sci., Série D* 280, 2301-2304.
- _____ (1977): Microthermometry and chemical analysis of fluid inclusions from the Rabbit Lake uranium deposit, Saskatchewan, Canada. *J. Geol. Soc. London* 134, 392.
- _____ & JAFFREZIC, H. (1977): Analyses chimiques des saumures des inclusions du quartz et de la dolomite du gisement d'uranium de Rabbit Lake (Canada). Aspect méthodologique et importance génétique. *Compte Rendu Acad. Sci. Paris, Série D* 284, 113-166.
- _____, POTY, B. & SHEPPARD, S.M.F. (1980): Contribution to some Saskatchewan uranium deposits mainly from fluid inclusion and isotopic data. In *Uranium in the Pine Creek Geosyncline*. International Atomic Energy Agency, Vienna, 639-654.
- RAMAEKERS, P. (1981): Hudsonian and Helikian basins of the Athabasca region, northern Saskatchewan. *Geol. Surv. Can. Pap.* 81-10, 219-233.
- SARACOGLU, N., WALLIS, R.H., BRUMMER, J.J. & GOLIGHTLY, J.P. (1983): The McClean uranium deposits, northern Saskatchewan - discovery. *Can. Inst. Mining Metall. Bull.* 76, 63-79.
- SIBBALD, T.I.I., HOEVE, J., RAMAEKERS, P. & LEWRY, J.F. (1981): Saskatchewan uranium field trip guide. In *Field Guides to Geology and Mineral Deposits*, Calgary, 1981 (R.I. Thompson & D.G. Cook, eds.). Geol. Assoc. Can., Waterloo, 121-142.
- TAKENOUCHI, S. & KENNEDY, G.C. (1965): The solubility of carbon dioxide in NaCl solutions at high temperatures and pressures. *Amer. J. Sci.* 263, 445-454.
- TAYLOR, H.P., JR. (1979): Oxygen and hydrogen isotope relationships in hydrothermal ore deposits. In *Geochemistry of Hydrothermal Ore Deposits* (2nd ed., H.L. Barnes, ed.). Wiley-Interscience, New York.
- TRUESDELL, A.H. (1974): Oxygen isotope activities and concentrations in aqueous salt solutions at elevated temperatures: consequences for isotope geochemistry. *Earth Planet. Sci. Lett.* 23, 387-396.
- WALLIS, R.H., SARACOGLU, N., BRUMMER, J.J. & GOLIGHTLY, J.P. (1983): Geology of the McClean uranium deposits. In *Uranium Exploration in the Athabasca Basin, Saskatchewan, Canada* (E.M. Cameron, ed.). *Geol. Surv. Can. Pap.* 82-11, 71-110.
- _____, _____, _____ & _____ (1984): The geology of the McClean uranium deposits, northern Saskatchewan. *Can. Inst. Mining Metall. Bull.* 77, 69-96.
- _____, _____, _____ & _____ (1985): The geology of the McClean uranium deposits, northern Saskatchewan. In *Geology of Uranium deposits* (T.I.I. Sibbald & W. Petruk, eds.). *Can. Inst. Mining Metall. Spec. Vol. 32*, 101-131.
- WENNER, D.B. & TAYLOR, H.P., JR. (1971): Temperatures of serpentinization of ultramafic rocks based on O¹⁸/O¹⁶ fractionation between coexisting serpentine and magnetite. *Contr. Mineral. Petrology* 32, 165-185.
- WENNER, D.G. & TAYLOR, H.P., JR. (1973): Oxygen and hydrogen isotope studies of the serpentinization of ultramafic rocks in oceanic environments and continental ophiolite complexes. *Amer. J. Sci.* 273, 207-239.
- WILLIAMS, A.E. & MCKIBBEN, M.A. (1987): A brine interface in the Salton Sea geothermal system, California: mechanism of active ore formation. *Geol. Soc. Amer. Ann. Meet., Abstr. Programs* 19, No. 7, 890.

- WILSON, M.R., KYSER, T.K., MEHNERT, H.H. & HOEVE, J. (1987): Changes in the H-O-Ar isotope compositions of clays during retrograde alteration. *Geochim. Cosmochim. Acta* **51**, 869-878.
- WORSLEY, N. & FUZESY, A. (1979): The potash-bearing members of the Devonian Prairie Evaporite of southeastern Saskatchewan, south of the mining area. *Econ. Geol.* **74**, 377-388.
- WRAY, E.M., AYRES, D.E. & IBRAHIM, H.J. (1985): Geology of the Midwest uranium deposit, northern Saskatchewan. In *Geology of Uranium deposits* (T.I.I. Sibbald & W. Petruk, eds.). *Can. Inst. Mining Metall. Spec. Vol.* **32**, 54-66.

Received April 16, 1987; revised manuscript accepted October 16, 1987.

APPENDIX

Locations of samples for which data are given in Tables 2 and 4.

Recrystallized sedimentary clay layers in Athabasca sandstone away from known uranium mineralization

- 3017-145 Between McClean N1 and McClean SE; 118 m above unconformity
 367-487 2.5 km WNW of McClean Lake; 40 m above unconformity
 375-502 E. of Candy Lake; 0.5 m above unconformity
 331-244 Moffat Lake area; 5 km NE of the McClean deposits; 8 m above unconformity

Illite pseudomorphs of primary feldspar in altered basement ("regolith") away from mineralization

- 2037-599 Outside mineralization between McClean N3 and N4 pods
 3017-537.5 Between McClean N1 and McClean SE; 5.5 m below the unconformity
 367-677.5 2.5 km WNW of McClean Lake
 367-713.5 2.5 km WNW of McClean Lake
 371-603.5 E. of Candy Lake; 27 m below the unconformity
 331-379 Moffat Lake area, 5 km NE of the McClean deposits; 33.3 m below the unconformity

Secondary illite from the hydrothermal alteration halo and from the "bleached" facies of uranium mineralization

- 188-541 McClean N1A
 2038-529 McClean N1A
 2045-523 McClean N1A
 180-527 McClean N1B
 2058-550 McClean N2
 2009-526 McClean N2
 2065-375 McClean N2
 2071-486 McClean N2
 207-533 McClean N2
 2019-541 McClean N3
 2076-487 McClean N3
 232-513 McClean N4
 1136-499 McClean SE
 1208-458 McClean SW

Typical unmineralized Athabasca sandstone

- 2038-259.5 McClean N1A
 1004-407 McClean SW
 1186-460 McClean SW
 1001-256 NE of Candy Lake
 331-87 Moffat Lake area 5 km NE of the McClean deposits

Fine grained disseminated siderite from the sulfide and arsenide facies of uranium mineralization

- 2049-534 McClean N1A
 2009-566 McClean N2
 2039-529 McClean N4
 1199-544 McClean SW
 1181-546.5 McClean SW
 1210-510 McClean SW
 1028-542 McClean SE
 1167-537 McClean SE
 to 542

Vein siderite from within and below mineralization

- 190-560 McClean N1A; within basement below mineralization; 9 m below unconformity
 172-510 McClean N1A; in mineralization; 6 m above unconformity
 3030-507.3 McClean N1A; near/within mineralization; 7 m above unconformity
 196-580 McClean N2; in basement below mineralization; 12 m below unconformity
 1201-543.5 McClean SW; near/within mineralization; 3.5 m above unconformity
 1214-565 McClean SE; below mineralization; 20 m below unconformity

Vein calcite below mineralization

- 2038-602 McClean N1A; coarse calcite in graphitic metasediment below mineralization; 22 m below the unconformity
 1172-598 McClean SW; calcite-quartz-sulfide veinlet in graphitic metasediment below mineralization; 13 m below the unconformity